GMAO RESEARCH BRIEF

June 2020

Ozone Data from Ultraviolet Satellite Measurements in GEOS Products

Krzysztof Wargan, Steven Pawson, Lawrence Coy and Austin Conaty

SUMMARY

Here, we describe the treatment of ozone observations from nadir ultraviolet (UV) sensors in the Global Earth Observing System (GEOS) data assimilation products generated at NASA's Global Modeling and Assimilation Office (GMAO). While the overarching goal is to use the most accurate data available, the selection of observations for different GEOS systems is also guided by product-dependent requirements: a long-term continuity for reanalyses; optimal quality for short-term analyses; and independence of data for outputs used by satellite instrument teams as priors in data retrieval algorithms. We highlight the key aspects of UV-derived ozone data used in three publicly available GEOS products: the Modern-Era Retrospective Analysis for Research and Applications (MERRA-2), GEOS Forward Processing systems (GEOS-FP), and the GEOS Forward Processing for Instrument Teams (GEOS-FPIT) product.

BACKGROUND

Atmospheric ozone is a critically important component of the Earth system. In the stratosphere, it absorbs most of the solar UV radiation at the shortest wavelengths, thus shielding the biosphere from its harmful effects and, indeed, allowing life to exist on land. Ozone absorption of solar radiation partly controls the thermal structure of the stratosphere and is a factor in shaping the large-scale stratospheric circulation. While about 90% of all ozone molecules reside in the stratosphere, tropospheric ozone is also of interest because of its role in the Earth's radiative budget and the deleterious impact it has on human health.

Introduction

Continuous satellite observations of Earth's atmospheric ozone began in the late 1970s. Over the past four decades, several remote measurement techniques have been developed for use with different satellite platforms. A series of nadir-viewing sensors that measure backscattered solar UV radiation provide the longest near-global ozone record. The distinct absorption spectra of ozone molecules are used to derive the total column ozone (equivalent to the total number of ozone molecules in a column of air between the surface and the top of the atmosphere; Figure 1) as well as partial columns (the ozone content within a set of vertically stacked layers).

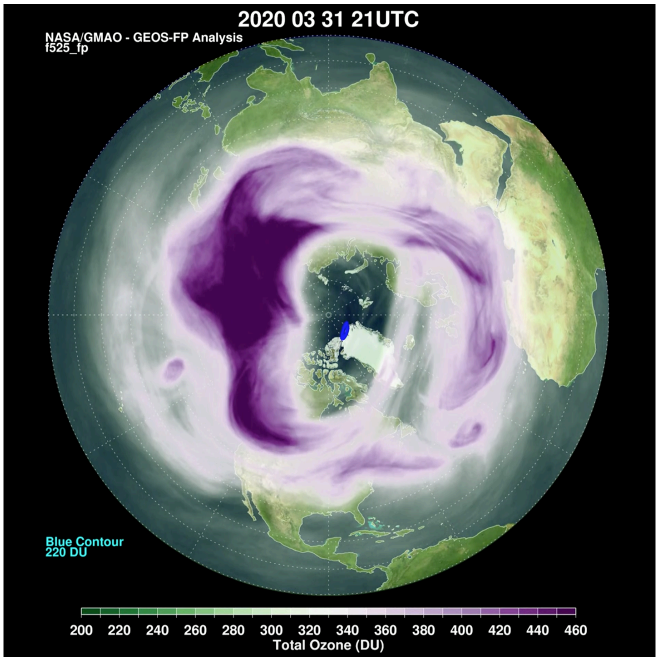

Figure 1. As a relatively short-lived gas, ozone is constantly produced, destroyed, and transported by winds, leading to the formation of complex time-varying patterns. This plot shows total column ozone over the Northern Hemisphere on 31 March 2020 at a record-breaking minimum. The image was produced from the GEOS-FP analysis. [View animated version.]

Assimilation of UV ozone observations in the GEOS systems

All officially released GEOS products include ozone output produced by assimilating satellite data. These products are used for scientific research, aid measurement campaigns, and provide prior information on the state of the atmosphere for satellite data retrievals. This research brief highlights important aspects of the use of ozone data from nadir UV observations in three types of GEOS products: MERRA-2 (Gelaro et al. 2017; https://gmao.gsfc.nasa.gov/reanalysis/MERRA-2/), GEOS-FP and GEOS-FPIT. General information about the latter two can be found on the GMAO website: https://gmao.gsfc.nasa.gov/weather_prediction/.

Table 1 and Figure 2 list the types of nadir UV ozone data assimilated in MERRA-2, GEOS-FP, and GEOS-FPIT, including the time periods for each observation type.

Observation type	Sensor	References	Satellite platforms	Usage in GEOS systems
Partial columns	SBUV	Bhartia et al. (2013)	Nimbus-7, NOAA-11,14,16,17,18,19	MERRA-2 (1980–2004) FP (20072014) GEOS-FPIT (2000–2020)
	OMPS-NP	Flynn et al. (2006)	Suomi-NPP, NOAA-20*	GEOS-FPIT (2020–present)
Total column	OMI	Levelt et al. (2018)	EOS Aura	MERRA-2 (2004–present) GEOS-FP (2012–present)
	OMPS-NM	Flynn et al. (2006)	Suomi-NPP, NOAA-20*	GEOS-FP (2019–present) GEOS-FPIT (2020–present)

Table 1 Acronyms: SBUV: Solar Backscatter UltraViolet radiometers; OMPS NP: Ozone Mapping Profiler Suite Nadir Profiler; OMPS NM: Ozone Mapping Profiler Suite Nadir Mapper; OMI: The Ozone Monitoring Instrument
* NOAA-20 data are not currently used but will be incorporated in the future

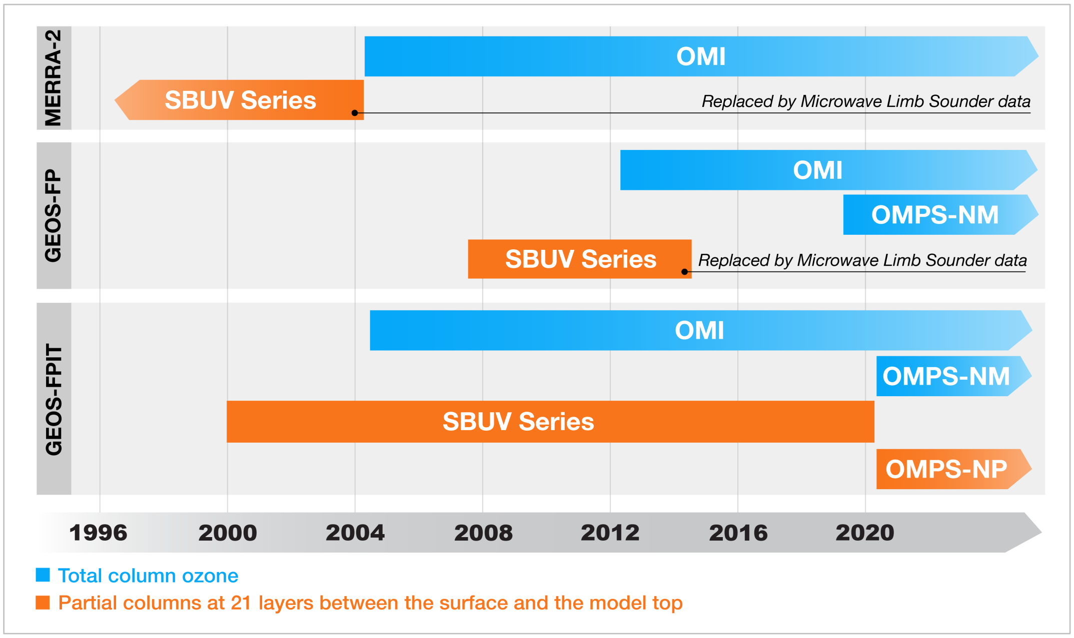

Figure 2. Timeline of UV nadir ozone data assimilated in MERRA-2 (top), GEOS-FP (middle), and GEOS-FPIT (bottom). The figure shows the periods of usage for each data type and GEOS product rather than availability of the observations. SBUV and OMPS data are available since 1979 and 2012, respectively and continue until the present.

The following sections describe the treatment of UV ozone data in MERRA-2, GEOS-FP, and GEOS-FPIT in more detail.

MERRA-2: an ozone climate data record

The MERRA-2 reanalysis provides a climate data record of global meteorological and ozone fields from 1980 to present. The MERRA-2 ozone observing system is relatively simple, with SBUV data assimilated between 1980 and 2004, and Aura observations (OMI and Microwave Limb Sounder, MLS) used afterward. This design was guided by the requirement that the best data available be used but that multiple observing system changes should be avoided when possible to limit spurious discontinuities in reanalysis output (Wargan et al. 2017).

Figure 3 shows deseasonalized MERRA-2 total column ozone anomalies with respect to the reanalysis climatology. A pronounced decline during the first two decades, especially evident in the extratropics, was caused by rapidly growing concentrations of ozone depleting substances, primarily chlorine-containing chlorofluorocarbons of industrial origin. As emissions of these compounds have been phased out following the Montreal Protocol and its amendments, stratospheric ozone has stopped decreasing and is expected to return to its pre-1980 levels later in the 21st century. Total column ozone also displays interannual variability associated with year-to-year variations in the atmospheric circulation and with the 11-year solar cycle, particularly clear in the tropics (Randel and Wu 2007). A deep minimum seen is the northern middle latitudes in the 1990s was associated with the aftermath of the eruption of Mt Pinatubo in 1991, which led to enhanced depletion of ozone in the lower stratosphere. While sulfate aerosols from the eruption were also present in the Southern Hemisphere, depletion there was masked by a dynamically driven ozone increase (Shepherd et al. 2014).

MERRA-2 ozone has been extensively evaluated against independent data and compared with that in other major reanalyses (Wargan et al., 2017; Davis et al., 2017). It is used by scientists in research areas ranging from long-term ozone variability and trends (Wargan et al., 2018; Orbe et al., 2020) to stratosphere-troposphere exchange (Jaeglé et al., 2017; Knowland et al., 2017).

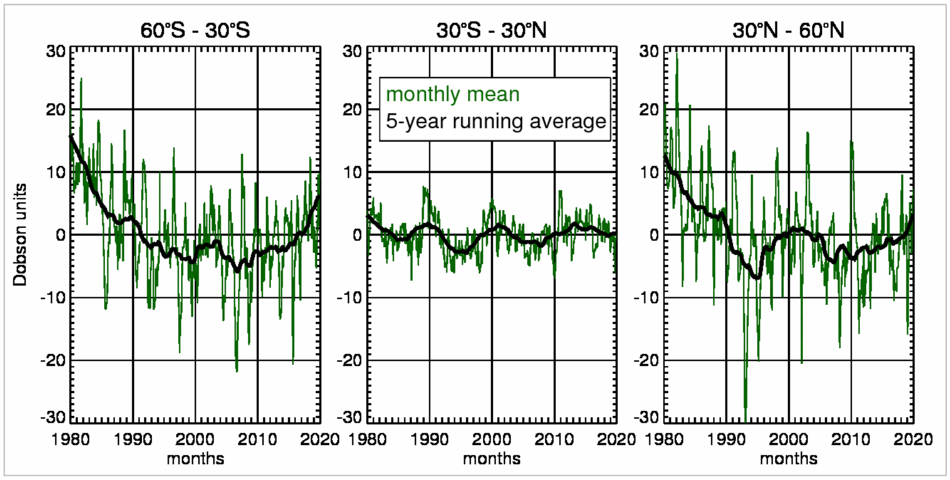

Figure 3. Total column ozone monthly anomalies calculated from MERRA-2 by subtracting the climatological seasonal cycle computed over the entire reanalysis period. The results are shown in three latitude bands: 60^{o}S–30^{o}S, 30^{o}S–30^{o}N, and 30^{o}N–60^{o}N. The high latitudes are omitted because the lack of coverage of the UV data in polar night limits our confidence in the MERRA-2 ozone there.

GEOS Forward Processing: ozone of the day

The GEOS-FP systems provide near real-time six-hourly analysis of global meteorological fields and ozone, along with five- and 10-day forecasts at high resolution (~12 km). Unlike MERRA-2, GEOS-FP is frequently upgraded with new model and data assimilation scheme developments and observations. The GEOS-FP product assimilates OMI (since 2012) and OMPS-NM (since 2019) total column ozone data, along with ozone profile observations from the MLS. Prior to 2015, the GEOS-FP systems also used partial ozone columns from the SBUV series (Figure 2).

Figure 4 shows the assimilated total ozone observations on 25 March 2020 at 18 UTC along with the resultant analysis and clearly illustrates how data assimilation propagates information from satellite observations in space to produce detailed global maps of total ozone. In the analysis, the large area of low ozone extending from Greenland and North America to the North Pole is reminiscent of the Antarctic ozone hole phenomena. This record-breaking depletion of ozone over the Arctic in spring 2020 resulted from an extremely cold and undisturbed polar vortex.

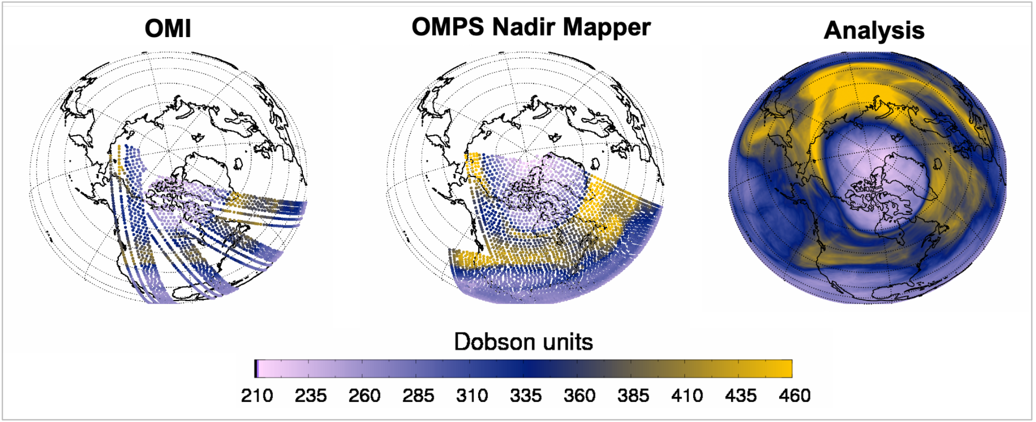

Figure 4. OMI (left) and OMPS-NM (middle) total column ozone observations assimilated into GEOS-FP during the 18 UTC assimilation window on 25 March 2020. The resulting assimilated total column ozone is shown on the right. The observations are screened for quality and spatially thinned prior to assimilation in order to reduce error autocorrelation.

GEOS Forward Processing for Instrument Teams: providing priors for satellite retrievals

GEOS-FPIT uses a stable version of the GEOS data assimilation system to produce near real-time and historical meteorological and ozone analyses. The current version of GEOS-FPIT is based on the MERRA-2 configuration. Because of specific requirements put forward by the main users of GEOS-FPIT, NASA Instrument Teams, MLS ozone and temperature are withheld from assimilation in GEOS-FPIT. The system assimilated SBUV and OMI (starting in 2004) ozone data until early 2020. In recent years, an orbital drift of the NOAA-19 satellite resulted in limited coverage provided by SBUV. In addition, the instrument has begun to exhibit signs of degradation leading to a spurious low bias near the tropical ozone maximum around 10 hPa. In order to limit the impact of instrument degradation on the GEOS-FPIT analysis, the SBUV assimilation was turned off and replaced by partial column data from OMPS-NP and total ozone measurements from OMPS-NM starting 23 April 2020.

Short tests conducted with both SBUV and OMPS configurations show that the introduction of the new data in GEOS-FPIT leads to a significant improvement of the assimilated ozone product compared with MLS data (Figure 5). The largest improvements are seen in the middle stratosphere, where a large dipole of positive (negative) bias in the southern high latitudes (Tropics) is largely reduced when OMPS data are assimilated. Note that due to the NOAA-19 satellite orbital drift, the southern high latitudes were not observed by SBUV in the period of this comparison. The analysis–MLS difference standard deviations are slightly reduced in the same region but increase in the northern high latitudes where ozone variability is also large during spring. This increase, as well as an ~0.5 ppmv positive bias in the northern hemisphere middle-stratospheric ozone, need further investigation.

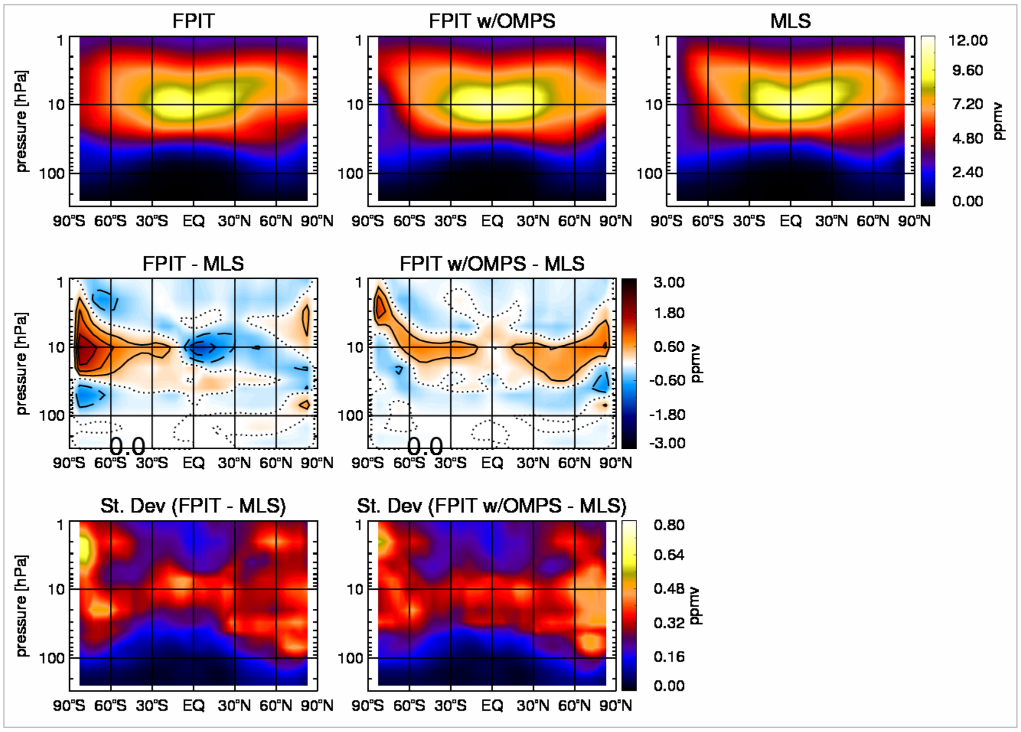

Figure 5. Zonal mean ozone from GEOS-FPIT with SBUV, GEOS-FPIT with OMPS and from MLS data between 1 and 10 April 2020 (top). The middle panel shows the relative zonal mean differences with MLS for the same period. The contour spacing is 0.5 ppmv. Bottom: standard deviations of analysis – MLS differences.

Further Work

The OMPS-NP and NM sensors are currently flying on the Suomi-NPP and NOAA-20 satellites, with future missions planned on subsequent JPSS platforms. In addition, high vertical resolution ozone measurements are provided by the OMPS Limb Profiler (OMPSLP) sensor on Suomi-NPP. OMPS-LP can be successfully assimilated into the GEOS data assimilation system, providing a valuable substitution for MLS in the future (Wargan et al. 2020). The OMPS sensors are projected to provide quality ozone data well into the 2030s. All these new data will be evaluated and incorporated into the GEOS products, including future GMAO reanalyses. In another line of development, the GMAO will test the feasibility of incorporating historical nadir UV data, including those from the European Global Ozone Monitoring Experiment–2 sensors flying on three European Metop satellites, as well as past OMPS observations extending back to 2012. If shown beneficial, these data will also be included in future reanalyses and the next generation of GEOS-FPIT.

References

Bhartia, P. K., R. D. McPeters, L. E. Flynn, S. Taylor, N. A. Kramarova, S. Frith, B. Fisher, and M. DeLand, 2013: Solar Backscatter UV (SBUV) total ozone and profile algorithm, *Atmos. Meas. Tech.*, **6**, 2533–2548, https://doi.org/10.5194/amt-6-2533-2013.

Davis, S. M., M. I. Hegglin, M. Fujiwara et al., 2017: Assessment of upper tropospheric and stratospheric water vapor and ozone in reanalyses as part of S-RIP. *Atmos. Chem. Phys.,* **17***,* 12,743-12,778, https://doi.org/10.5194/acp-17-12743-2017

Flynn, L. E., C. J. Seftor, J. C. Larsen, and P. Xu, 2006: The Ozone Mapping and Profiler Suite, in: *Earth Science Satellite Remote Sensing*, edited by: Qu, J. J., Gao, W., Kafatos, M., Murphy, R. E., and Salomonson, V. V., Springer, Berlin, 279-296, doi:10.1007/978-3-540-37293-6

Gelaro, R., W. McCarty, M. J. Suarez et al., 2017: The Modern-Era Retrospective Analysis for Research and Applications, Version-2 (MERRA-2). *J. Climate*, **30**, 5419-5454. https://doi.org/10.1175/JCLI-D-16-0758.1

Jaeglé, L., R. Wood and K. Wargan, 2017: Multiyear composite view of ozone enhancements and stratosphere-to-troposphere transport in dry intrusions of northern hemisphere extratropical cyclones. *J. Geophys. Res.: Atmos.*, **122**, 13,436-13,457. https://doi.org/10.1002/2017JD027656

Knowland, K. E., L. E. Ott, B. N. Duncan and K. Wargan, 2017: Stratospheric intrusion-influenced ozone air quality exceedances investigated in the NASA MERRA-2 reanalysis. *Geophys. Res. Lett.*, **44**, 10,691-10,701. https://doi.org/10.1002/2017GL074532

Levelt, P. F., J. Joiner, J. Tamminen, J. P. Veefkind, P. K. Bhartia, D. C. Stein Zweers, B. Duncan et al., 2018: The Ozone Monitoring Instrument: overview of 14 years in space, *Atmos. Chem. Phys.*, **18**, 5699-5745, https://doi.org/10.5194/acp-18-5699-2018

Orbe, C., K. Wargan, S. Pawson and L. D. Oman, 2020: Mechanisms linked to recent ozone decreases in the Northern Hemisphere lower stratosphere. *J. Geophys. Res.: Atmos.*, **125**, e2019JD031631. https://doi.org/10.1029/2019JD031631

Randel, W. J., and F. Wu, 2007: A stratospheric ozone profile data set for 1979-2005: Variability, trends, and comparisons with column ozone data. *J. Geophys. Res.*, **112**, D06313, https://doi.org/10.1029/2006JD007339.

Shepherd, T., D. Plummer, J. Scinocca et al., 2014: Reconciliation of halogen-induced ozone loss with the total-column ozone record. *Nat. Geosci.,* **7,** 443-449. https://doi.org/10.1038/ngeo2155

Wargan, K., G. J. Labow, S. M. Frith, S. Pawson, N. J. Livesey and G. S. Partyka, 2017: Evaluation of the Ozone Fields in NASA's MERRA-2 Reanalysis. *J. Clim.*, **30**, 2961-2988. https://doi.org/10.1175/JCLI-D-16-0699.1

Wargan, K., N. Kramarova, B. Weir, S. Pawson and S. Davis, 2020: Toward a reanalysis of stratospheric ozone for trend studies: Assimilation of the Aura Microwave Limb Sounder and Ozone Mapping and Profiler Suite Limb Profiler data. *J. Geophys. Res.: Atmos.*, **125**, e2019JD031892. https://doi.org/10.1029/2019JD031892

Wargan, K., C. Orbe, S. Pawson, J. R. Ziemke, L. D. Oman, M. A. Olsen et al., 2018: Recent decline in extratropical lower stratospheric ozone attributed to circulation changes. *Geophys. Res. Lett*, **45**, 5166-5176. https://doi.org/10.1029/2018GL077406